Polymer 50 (2009) 2294–2303

Contents lists available at ScienceDirect

Polymer

journal homepage: www.elsevier.com/locate/polymer

# Characterization of the effect of the filler dispersion on the stress relaxation behavior of carbon black filled rubber composites

H.H. Le, S. Ilisch, H.-J. Radusch*

*Center of Engineering Sciences, Martin Luther University Halle-Wittenberg, D-06099 Halle (Saale), Germany*

ARTICLE INFO

*Article history:*
Received 18 November 2008
Received in revised form
26 February 2009
Accepted 27 February 2009
Available online 27 March 2009

*Keywords:*
Stress relaxation
Rubber composites
CB network

ABSTRACT

In the present work a new evaluation method for the characterization of the stress relaxation behavior of rubber–carbon black (CB) composites is presented. Using the chart of the online measured electrical conductance received from the recording equipment in the mixing chamber different rubber–CB composites with well defined state of the CB network have been produced for the stress relaxation investigation. The development of CB dispersion degree and the rubber-layer bonded on the CB surface have been characterized systematically using the method of the online measured electrical conductance and the thermogravimetric analysis of rubber–filler gel. The analysis of the stress relaxation curves is based on the division of the initial stress into several stress components and the consideration of the structure of the composites as a combination of different networks. The contribution of the stress component to the corresponding network is the focus of the present work. Based on the systematic variation of material parameters and test conditions we could divide the applied stress into six stress components which are originated from the rubber matrix and CB. It is obvious that the debonding of the rubber-layer from the CB surface and the collapse of a part of the CB network can be described by the relaxing stress component $\Delta\sigma^{CB(rubber\text{-}layer)}$ and $\Delta\sigma^{CB(network)}$, respectively. The non-relaxing stress components $\sigma_{\infty}^{CB(rubber\text{-}layer)}$ and $\sigma_{\infty}^{CB(network)}$ are dependent on the amount of the time-stable bonding in the rubber-layer and the stable part of the CB network. The mechanical performance of the composites and especially the time and temperature dependent mechanical behavior could be specifically modified by CB addition.



## 1. Introduction

The mixing of carbon black (CB) in rubber composites improves their performance-related properties [1]. Depending on the material parameters and mixing technology CB undergoes different dispersion states, from large agglomerates to small aggregates. In order to obtain optimal vulcanizate properties, CB must be sufficiently dispersed in the mixture [2]. Poor macrodispersion which is determined by agglomerates with a size larger than 6 μm is responsible for the decrease in ultimate tensile strength, breaking and tearing energy, or fatigue resistance. Small agglomerates and aggregates (microdispersion) influence the end use performance of many vehicle systems resulting in lower hysteresis properties and higher resistance to tearing, cut growth and abrasion [3].

The time and temperature dependent mechanical behavior of filled vulcanizates has been investigated extensively by many researchers [4–8]. Ronan [5] proposed a method to separate physical and chemical relaxation processes. The basis of the method is to evaluate the continuous relaxation time spectrum for each test temperature in order to separate the relaxation processes. Vennemann [6] developed a new test method, namely Temperature Scanning Stress Relaxation (TSSR) to characterize the thermo-mechanical behavior of filled vulcanizates. During TSSR tests, the temperature increases at a constant rate. During heating the decrease of the applied stress was explained as a result of different processes like break-down of filler network, desorption of bound rubber and thermo-oxidative chain scission. Using dynamic mechanical analysis and dielectric relaxation spectra on CB filled ethylene–propylene–rubber (EPDM) and chlorobutyl vulcanizates Mahapatra and Sridhar [7,8] found that debonding of the rubber chains in the vicinity of filler is essential for stress relaxation behavior. However, our comprehensive literature research revealed, in those works CB was always considered as well dispersed, the effect of CB dispersion degree has not been characterized so far.

In order to evaluate the stress relaxation behavior, among different models the two-component model has been frequently used. On its basis the relaxation curve $\sigma(t)$ can be separated into

* Corresponding author. Tel.: +49 (3461) 46 2791/3792; fax: +49 3461 46 3891.
*E-mail address:* hans-joachim.radusch@iw.uni-halle.de (H.-J. Radusch).

0032-3861/$ – see front matter © 2009 Elsevier Ltd. All rights reserved.
doi:10.1016/j.polymer.2009.02.051

two components, a relaxing curve $\Delta\sigma(t)$ and a non-relaxing stress component $\sigma_\infty$ [9–12]:

$$\sigma(t) = \Delta\sigma(t) + \sigma_\infty \quad (1)$$

If $t \to \infty$, the initial stress value $\sigma$ is the sum of the relaxing stress component $\Delta\sigma$ and the non-relaxing stress one $\sigma_\infty$:

$$\sigma = \Delta\sigma + \sigma_\infty \quad (2)$$

According to Seeger [9,10] the relaxing stress component $\Delta\sigma$ is called thermally activated stress component, because it acts on short-range obstacles, which can be overcome by stress aided thermal activation. It depends on the plastic deformation rate and temperature according to Eyring's rate theory [11]. In contrast to the relaxing stress component $\Delta\sigma$, the non-relaxing stress component $\sigma_\infty$ is called athermal stress component. It is originated from long-range stress fields, which cannot be overcome by thermal activation.

On the basis of the two-component model we have developed an evaluation method for the characterization of the stress relaxation behavior of multi-component polymer systems [13]. The basis idea is to consider the investigated system as a combination of different networks. A systematic variation of material parameters and test conditions allows separating the initial stress $\sigma$ into different components and to assign them to the according networks in the system. The proposed method was successfully applied for the evaluation of the time and temperature dependent deformation behavior of the unfilled thermoplastic elastomers TPE [13] and the oil extended TPE as well [14].

Recently, the methods of the online measured electrical conductance and the thermogravimetric analysis (TGA) of the rubber–filler gel delivered comprehensive knowledge about the wetting behavior of CB surface, the infiltration processes of the rubber chains into the filler agglomerate voids and the dispersion kinetics of CB agglomerates as well as the development of the CB network during the mixing process [15,16]. A description of the morphology development of the filled vulcanizates and the characterization of its effect on the stress relaxation behavior by use of the proposed evaluation methods are the focus of the present work.

## 2. Materials and experimental

### 2.1. Materials

Hydrogenated acrylonitrile butadiene rubber (HNBR) Zetpol 2030L (Zeon Deutschland) with acrylonitrile content of 36%, hydrogenation of 85% and Mooney viscosity at 100 °C of 50–65 ML was used as the polymer matrix. Carbon black EC600 (Akzo Nobel) was used as a filler. Its structure and specific surface area characterized by the dibutyl phthalate (DBP) number and nitrogen adsorption (NSA) were 500 ml/100 g and 1400 $m^2/g$, respectively. Peroxide Luperox 101 (Atofina Chemicals) was used as a curing agent. A concentration of 2% of peroxide was kept constant for all composites.

### 2.2. Mixing technique and sample preparation

Mixing experiments were performed by a Poly Lab System Rheocord 300 p with a 75 $cm^3$ mixing chamber Rheomix 610 p (Thermo Haake). The initial chamber wall temperature was kept constant at 50 °C, the rotor speed was 50 rpm, and the fill factor 0.7. First, rubber was masticated for 2 min containing peroxide and then CB was added. CB concentration of 10 phr was kept constant for all composites. An unfilled vulcanizate (V) was prepared as a reference system.

A conductivity sensor has been installed in the chamber of the internal mixer to measure the electrical conductance signal of the mix volume between the sensor and the chamber wall as used in [15]. The construction and position of the conductivity sensor were modified correspondingly in order to detect the conductance signal of the investigated system. In order to receive rubber–CB composites with defined CB dispersion, the mixing time was varied by taking into account the electrical conductance–time characteristics as done in our previous work [17].

After discharge from the mixer, all samples were cross-linked at a temperature of 145 °C and pressure of 70 bar and $t_{90}$ using a compression moulding device P200 (Collin) to get sheets of 1 mm thickness for stress relaxation experiments.

### 2.3. Morphology characterization, thermal and mechanical testing

#### 2.3.1. Optical microscopy

Optical microscopy has been used to characterize the CB dispersion. This method was described by Stumpe and Railsback [18] and modified by us. We produced gloss cuts by cutting stretched samples having a dimension of 1 mm × 5 mm × 20 mm by a razor blade at room temperature and examine the cut surfaces by light microscope. If the surface of the cut contains CB agglomerates or aggregates, the light scatters at this place and its area appears dark. With an image analysis program one can calculate the area of visible CB regions using Eq. (3) according to ASTM 2663 [19].

$$D = \left(1 - \frac{A}{A_0}\right) \times 100\% \quad (3)$$

$A$ is the sum of all areas of agglomerates with a diameter larger than 6 μm, $A_0$ is the area of the investigated image. A dispersion index of 100% means, that no agglomerate size larger than 6 μm could be found in the cut surface. From every sample six micrographs were made and from every micrograph six images were analyzed.

#### 2.3.2. Atomic force microscopy

Investigations of microdispersion were carried out by a Universal Scanning Probe Microscope (AFM) (Ambios), operated in intermittent mode with a scan-head of 5 μm. Samples were produced by cutting in a cryo-chamber CN 30 of a rotary microtom HM 360 (Microm) with a diamond knife at −120 °C.

#### 2.3.3. Extraction experiments of uncured mixtures for determination of the rubber-layer L bonded on the surface of CB

On the basis of our developed method [16,20] the characterization of the wetting behavior of CB by rubber chains was realized. When CB is mixed with a rubber, a part of the rubber chains will be bonded with the active centers which are available on the surface of CB. During the extraction experiment of the filled composites with acetone, the rubber-layer bonded on the CB surface remains in the rubber–filler gel. In contrast to the bound rubber often reported in literature we calculate the rubber-layer $L$ as a part of the rubber–CB gel according to Eq. (4) [16,20].

$$L = \frac{m_2 - m_1 c_R}{m_2} \quad (4)$$

The mass $m_1$ corresponds to the composite before extracting; it is the sum of the mass of the undissolvable rubber, the mass of the soluble rubber and of CB. $m_2$ is the mass of the rubber–filler gel, which is the sum of the undissolvable rubber and the mass of CB. $c_R$ is the mass concentration of CB in the composite. For the experimental work 0.25 g of the uncured mixture were stored at room temperature in 100 ml acetone. After three days the rubber–filler

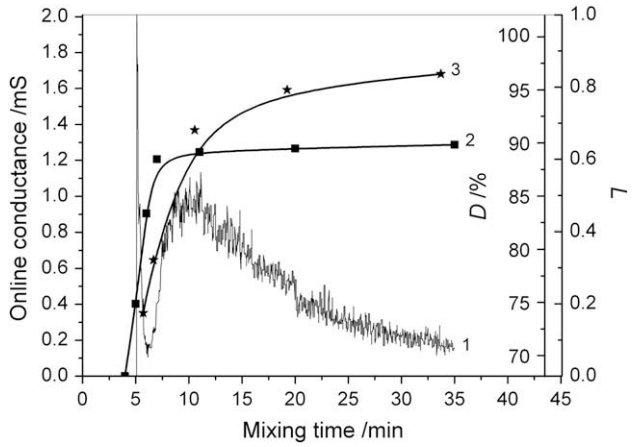


**Fig. 1.** Online conductance (curve 1), rubber-layer $L$ (curve 2) and the CB dispersion degree $D$ (curve 3) in dependence on the mixing time.

gel was taken out and dried in an oven at 80 °C for 2 h up to a constant mass. The value of $L$ varies between 0 and 1.

#### 2.3.4. Extraction experiments of cured vulcanizates and composites

Extraction experiments were performed with cured samples by equilibrating them in acetone at room temperature for 48 h. Because the volume fraction of CB of 4.34 vol.% is considered as negligible, the swelling degree $Q$ and the cross-linked part $C$ were simply calculated using Eq. (5).

$$Q = \frac{W_{sw} - W_i}{W_i} \times 100\%; \quad C = \frac{W_{dr}}{W_i} \times 100\% \tag{5}$$

where $W_i$ is the weight of the rubber sample before immersion into the solvent, $W_{sw}$ and $W_{dr}$ are the weights of the sample in the swollen state and after dried in an oven at 80 °C for 2 h from its swollen state, respectively.

#### 2.3.5. Stress relaxation experiments

Stress relaxation experiments were performed using a testing machine 1425 with a 2 kN measuring head (Zwick/Roell). The machine was equipped with a heating chamber enabling a long-term constancy of the temperature. Relaxation curves for all samples were recorded at a draw ratio $\lambda = 1.5$ (strain $\varepsilon = 50$ %) within the temperature range from 30 °C to 110 °C over a period of about 3 h. A strain rate of 100% $min^{-1}$ was kept constant. No steady state of stress values was observed even after 3 h. Therefore, an extrapolation method proposed by Li [21] was used to determine the non-relaxing stress component $\sigma_\infty$.

## 3. Results and discussion

### 3.1. Characterization of the morphology development of the rubber–CB composites along the mixing time

In Fig. 1 the online conductance of a rubber–CB composite, the dispersion degree $D$ and the rubber-layer $L$ are presented in dependence on the mixing time. The online conductance curve shows a typical shape as received in our previous work [15]. The minimum of the conductance is observed at about 7 min and the local maximum at 11 min. A small quantity of the mixture was taken out during the mixing process at different mixing times (7, 11, 20 and 35 min) and investigated by different testing methods including the optical microscopy, atomic force microscopy, and extraction experiments.

Several CB agglomerates can be observed in the images made by optical microscopy presented in Fig. 2 (macrodispersion). The strongest change of the size and number of CB agglomerates is determined in the range between 7 min and 11 min. The macro-dispersion $D$, as the measure describing the change of the CB agglomerate sizes, was determined from the images according to Eq. (3) and is presented in Fig. 1 (curve 3). As discussed in our previous work [15] the macrodispersion and the online conductance correlate closely to each other in the period between the minimum and the local maximum. After passing the local maximum the conductance decays rapidly but the macrodispersion still increases slightly. The main reason for the decrease of conductance is related to the distribution of small aggregates throughout the matrix, which can be described by the microdispersion.

The composites taken out at 7, 11, 20 and 35 min are denoted as C79, C91, C95 and C97, respectively. The number behind the label C indicates the degree of the macrodispersion $D$. The development of the network of the CB aggregates correlating directly with the chart of the online conductance is presented by the AFM images in Fig. 3 (microdispersion).

At 7 min (Fig. 3a) the AFM image of the composite C79 shows, that the outer layer of the CB agglomerate (bounded by a white line) is eroded into a number of small aggregates which are surrounding the agglomerates as model-like described by the *infiltration* and *onion model* [22–25]. Since the mixing time is still short, the small aggregates are not yet distributed far away from the boundary of the large agglomerate. The CB network at this state is mainly built-up by the large agglomerates. Some unfilled rubber regions still prevent the build-up of the CB network and keep the composite still low-conductive. When the mixing time increases up to 11 min (C91, Fig. 3b) the size of agglomerates decreases very fast, while the number of the small aggregates increases rapidly. The small aggregates and the remaining agglomerates build a continuous network which facilitates the motion of electrons and thus the

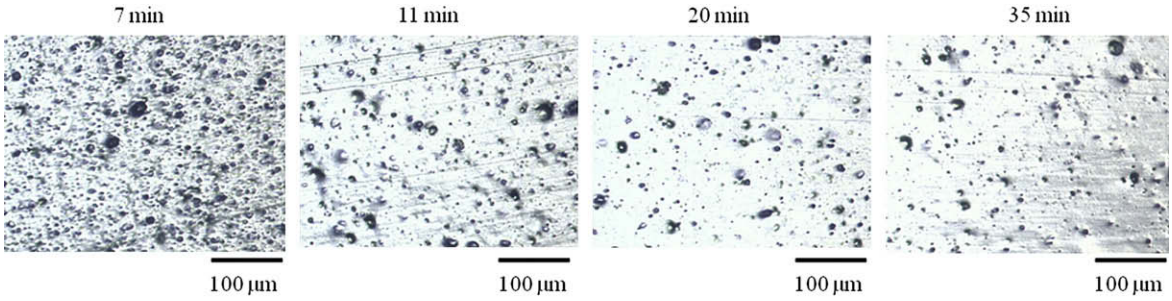


**Fig. 2.** Images of the composites taken out at different mixing times.

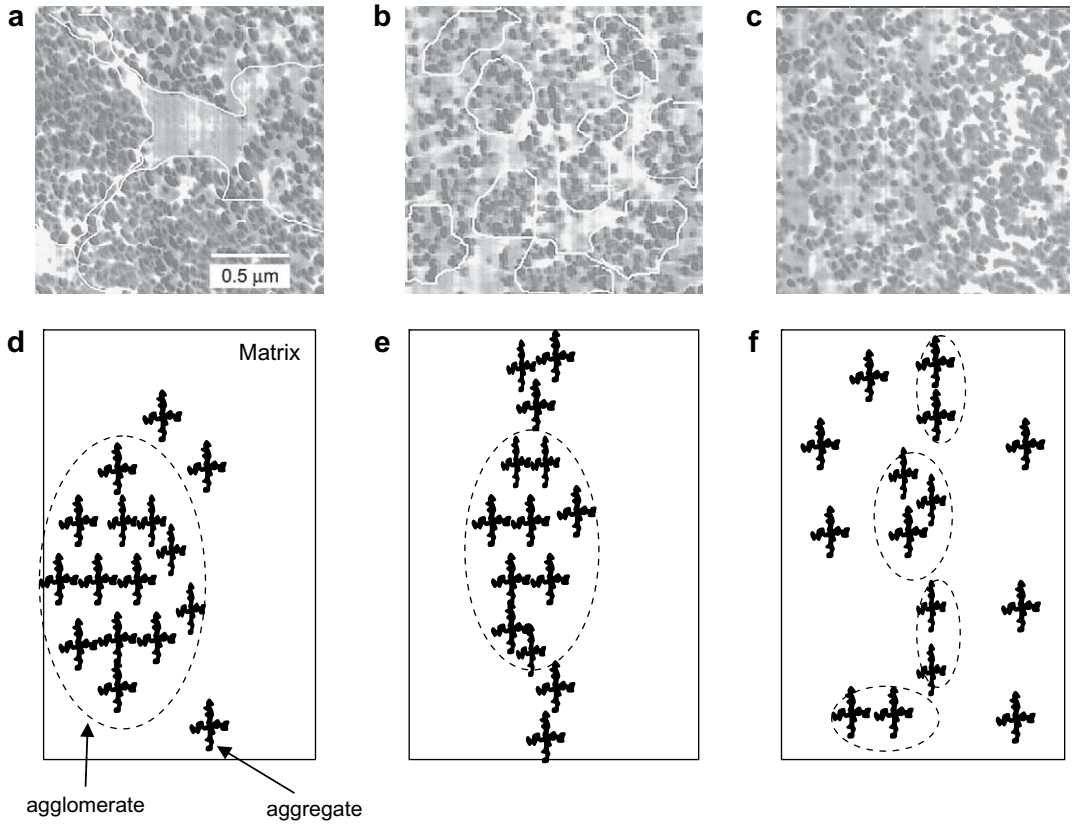


**Fig. 3.** Development of the CB network along the mixing time, AFM images of C79 (7 min) (a), C91 (11 min) (b) and C97 (35 min) (c), schematic illustrations of C79 (d), C91 (e) and C97 (f).

online conductance increases to a local maximum. Passing the mixing time of 11 min the dispersion processes slow down while the distribution processes of the small aggregates throughout the matrix become dominant that weakens the CB network and causes a decay of the online conductance in this period (C97, Fig. 3c). The development of the CB network can be illustrated schematically as seen in Fig. 3d,e and f.

The wetting process of the CB surface by the rubber chain is illustrated by the rubber-layer *L* in Fig. 1 (curve 2). Rubber-layer *L* is determined as the rubber portion that cannot be separated from the filler when the filled compound is extracted in a good solvent, such as acetone, during a certain period of time. The larger the amount of polymer that stays on the CB surface, the better the polymer–filler interaction which has also been related to improved final properties. The interactions which keep the polymer on the CB surface from being dissolved by the solvent can be explained from two different views: On the one hand, bound rubber has been regarded to be caused merely by adsorption effects in which van der Waals forces and chemisorption play the main role [26]. On the other hand, bound rubber formation has been attributed to a chemical process. This process was assumed to be caused by reactions of the rubber with functional groups present on the surface of CB [27]. Also rubber radicals formed by mechanical–chemical degradation during mixing can react with active sites newly formed on CB, for example due to the break-down of its structure during mixing [28]. In Fig. 1 the rubber-layer *L* increases in line with conductance and dispersion in the early mixing state. According to the discussion made by Manas-Zloczower [23,24] about the infiltration and dispersion processes, rubber first will infiltrate the outer layer of CB and wets its surface. This CB layer is then peeled off and a new CB surface is created. The new CB surface is progressively wetted by rubber. Therefore the wetting and dispersion take place simultaneously. The rubber-layer *L*-time curve, which describes the wetting process, gets a plateau before the local maximum of online conductance is reached. This behavior is as similar as the one of the NR compounds filled with CB as found in our previous work [16,20].

Deduced from Fig. 1 the development of the rubber-layer *L* and the CB network which is reflected by the online conductance are presented in Fig. 4 in dependence on the CB dispersion *D*. Obviously the development of the rubber-layer *L* is already completed for all systems investigated in the present work. The CB network of the

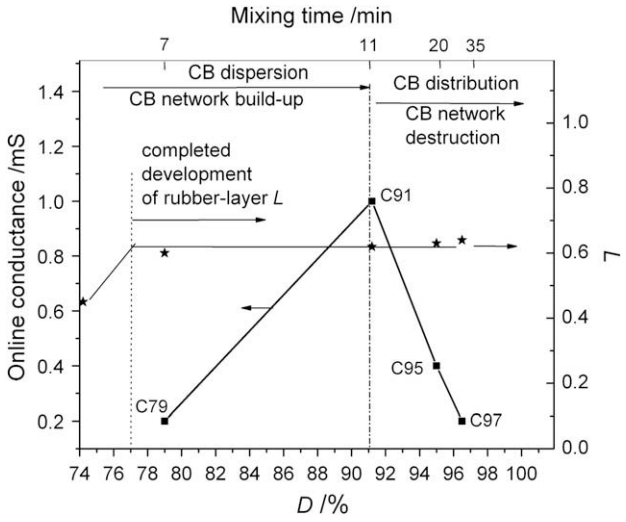


**Fig. 4.** Online conductance and rubber-layer *L* in dependence on CB dispersion degree *D*.

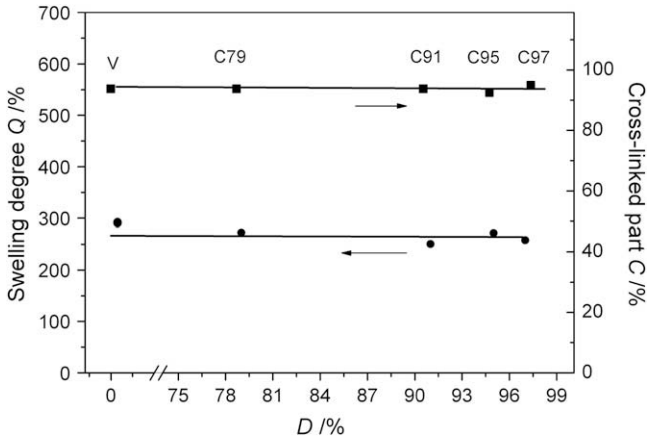


**Fig. 5.** Swelling degree $Q$ and cross-linked part $C$ of the unfilled vulcanizate V and the composites.

composite C79 is not yet developed and still consists of large agglomerates. With increasing CB dispersion the number of small aggregates becomes much higher. These small aggregates build a continuous CB network throughout the matrix of the composite C91. Through the distribution process the distance between small aggregates becomes larger, thus, the network in the composites C95 and C97 becomes looser and it becomes more easily to be destroyed by mechanical load.

The cross-link density of the rubber matrix of the investigated samples can be estimated by the swelling degree $Q$ and the cross-linked part $C$ of the rubber matrix as shown in Fig. 5.

The swelling degree $Q$ of about 280 wt.% and the amount of the cross-linked part $C$ of about 95 wt.% were found for the unfilled vulcanizate V and all the composites. That means the cross-link density of the composites is similar to that of the unfilled vulcanizate V and not dependent on the degree of CB dispersion. There is about 5 wt.% of the sample extracted which is related to the uncross-linked part of the rubber matrix.

### 3.2. Stress relaxation behavior

The stress relaxation curves of the unfilled vulcanizate V recorded at different temperatures are shown in Fig. 6a. With increasing test temperature the relaxation curves $\sigma^{V}(t)$ shift to a higher level that generally has been considered as a result of the entropy elastic forces [29]. The relaxation curves of the composite C91 measured at different test temperatures are presented in Fig. 6b. The addition of CB reinforces the rubber matrix and thus the relaxation curves $\sigma^{Comp}(t)$ of the composite lie at a higher level compared to $\sigma^{V}(t)$. In contrast to $\sigma^{V}(t)$ the curves $\sigma^{Comp}(t)$ shift downwards with increasing test temperature. It is remarkable, that the curve $\sigma^{Comp}(t)$ measured at 50 °C intersects the curves measured at higher temperatures. The reason can be the temperature induced change of the structure of the composites that will be explained later more in detail.

At the end region of the curve measured at high temperatures presented in Fig. 6a and b an acceleration of the relaxation rate is observed. That is related to the chemical degradation of the rubber chains, since no antioxidant was mixed into the investigated systems. In the present work, the effect of the chemical influences on the stress relaxation will be neglected. Without the chemical relaxation the stress will theoretically reach an end value – the non-relaxing stress component $\sigma_\infty$ – at the infinite time $t_\infty$. In order to determine the non-relaxing stress component $\sigma_\infty$ the extrapolation method proposed by Li [21] was used. He proposed that the relaxation rate $-d\sigma/dt$ becomes zero at the infinite time when all relaxation processes are finished. The principle of this method is representatively shown for the determination of $\sigma_\infty$ from the relaxation curves measured at 30 °C and 90 °C. In a diagram $-d\sigma/dt$ vs. $\sigma$ the extrapolation of the straight part of the curve measured at 30 °C (Fig. 7a) toward the $x$-axis intersects it at a certain value which is identified as $\sigma_\infty$.

The curve measured at 90 °C (Fig. 7b) shows some values deviating from the straight part of the curve which is attributed to chain degradation processes. Neglecting the chemical relaxation the extrapolation was done only for the straight part as shown in Fig. 7b.

According to Eq. (2) the initial stress $\sigma^{V}$ of the unfilled vulcanizate V is divided into the relaxing stress component $\Delta\sigma^{V}$ and the non-relaxing stress component $\sigma^{V}_\infty$ as presented in Fig. 8a. The relaxing stress component $\Delta\sigma^{V}$ is originated by the relaxation process of the entanglements and the uncross-linked rubber part determined from the swelling measurement. In the entropy elastic state above the glass transition temperature the relaxing stress component $\Delta\sigma^{V}$ remains nearly unaffected by the test temperature.

The non-relaxing stress component $\sigma^{V}_\infty$ is caused by the deformation of the network formed by the chemical cross-links. It increases with increasing temperature according to the entropy elasticity theory described by Eq. (6) [29].

$$\sigma^{V}_\infty = \left(\lambda - \lambda^{-2}\right)E^{V}_\infty = \left(\lambda - \lambda^{-2}\right)\frac{3\rho kT}{M_C} \tag{6}$$

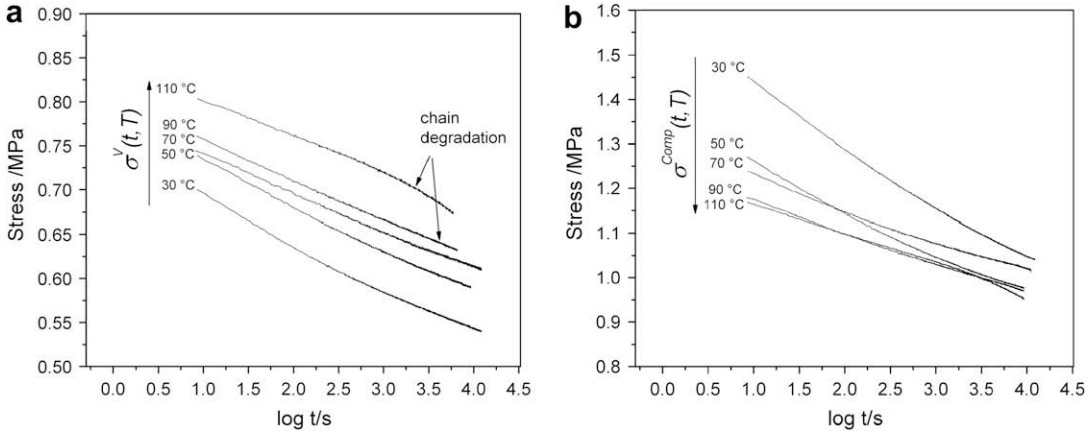


**Fig. 6.** Stress relaxation curves of the unfilled vulcanizate V (a) and the composite C91 (b) recorded at different test temperatures.

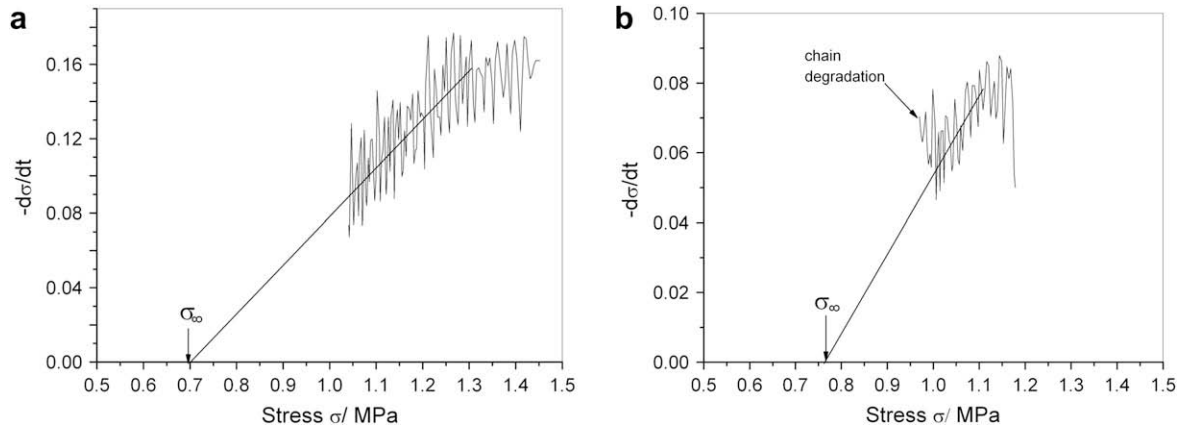


**Fig. 7.** Determination of the non-relaxing stress component $\sigma_\infty$ of the composite C91 using the extrapolation method proposed by Li [21] at 30 °C (a) and 90 °C (b).

In Eq. (6) the rubber elastic modulus $E^V_\infty$ is calculated from the non-relaxing stress component $\sigma^V_\infty$ and the draw ratio $\lambda$. It depends also on the density $\rho$, the Boltzmann constant $k$, the absolute temperature $T$ and the average molecular weight between cross-links $M_C$.

An average molecular weight between the cross-links $M_C$ of about 7000 g/mol was found as displayed in Table 1. $M_C$ is independent of the test temperature.

In Fig. 8b the initial stress $\sigma^{Comp}$, the relaxing and non-relaxing stress components $\Delta\sigma^{Comp}$ and $\sigma^{Comp}_\infty$, respectively, of the composite C91 are presented in dependence on the test temperature. Similar to the non-relaxing stress component of the unfilled vulcanizate $\sigma^V_\infty$ the non-relaxing stress component of the composite $\sigma^{Comp}_\infty$ increases with temperature but in contrast to $\Delta\sigma^V$ the relaxing stress component $\Delta\sigma^{Comp}$ decreases strongly due to the temperature dependent acceleration of any relaxation processes which have not yet been identified by now.

From the assumption that all the networks available in the composite are combined in a parallel circuit [30], the relaxing and non-relaxing stress components of the composite $\Delta\sigma^{Comp}$ and $\sigma^{Comp}_\infty$, respectively, can be determined by $\Delta\sigma^M$ and $\sigma^M_\infty$ generated by the composite matrix and $\Delta\sigma^{CB}$ and $\sigma^{CB}_\infty$ generated by CB addition according to Eqs. (7) and (8).

$$\Delta\sigma^{Comp} = \Delta\sigma^M + \Delta\sigma^{CB} \tag{7}$$

and

$$\sigma^{Comp}_\infty = \sigma^M_\infty + \sigma^{CB}_\infty \tag{8}$$

Based on the fact that the cross-link density of the unfilled vulcanizate V and the composite matrix are the same, the relaxing and non-relaxing stress components $\Delta\sigma^M$ and $\sigma^M_\infty$ generated by the composite matrix can be calculated from $\Delta\sigma^V$ and $\sigma^V_\infty$ of the unfilled vulcanizate V with respect to the volume concentration $\varphi$ of the filler using Eqs. (9) and (10).

$$\Delta\sigma^M = (1-\varphi)\Delta\sigma^V \tag{9}$$

and

$$\sigma^M_\infty = (1-\varphi)\sigma^V_\infty \tag{10}$$

The relaxing stress component $\Delta\sigma^{CB}$ of CB was calculated using Eqs. (7) and (9) and representatively presented in Fig. 9 for the composite C91. It decreases with increasing test temperature. The relaxing stress component $(1-\varphi)\Delta\sigma^V$ of the matrix is insignificantly dependent on the temperature, thus the decrease of the relaxing stress component $\Delta\sigma^{CB}$ of CB is the main reason for the decrease of the relaxing stress component $\Delta\sigma^{Comp}$ of the composite presented in Fig. 8b.

The non-relaxing stress component $\sigma^{CB}_\infty$ of CB of the composite C91 calculated using Eqs. (8) and (10) is presented in Fig. 10. Because the non-relaxing stress component $\sigma^{CB}_\infty$ remains unchanged with increasing temperature, the increase of $\sigma^{Comp}_\infty$ with temperature is a result of the chemical network of the matrix $(1-\varphi)\sigma^V_\infty$ under influence of the entropy elastic forces.

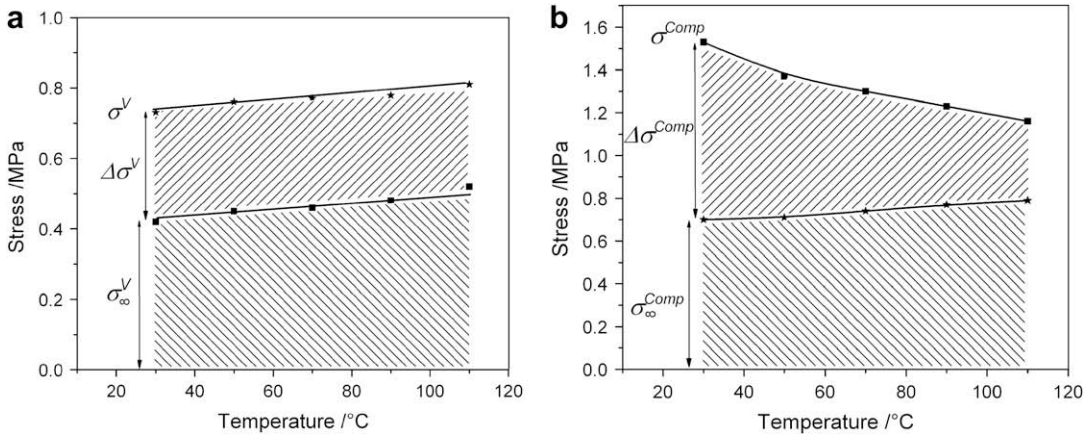


**Fig. 8.** Temperature dependence of the initial stress $\sigma$, relaxing stress component $\Delta\sigma$ and non-relaxing stress component $\sigma_\infty$ of the unfilled vulcanizate V (a) and composite C91(b).

**Table 1**
Parameters of Eq. (6) for the unfilled vulcanizate V.

| Temp | 30 °C | 50 °C | 70 °C | 90 °C | 110 °C |
|---|---|---|---|---|---|
| $\sigma_\infty^V$ | 0.42 | 0.45 | 0.465 | 0.495 | 0.522 |
| $E_\infty^V$ | 0.396 | 0.425 | 0.439 | 0.467 | 0.492 |
| $M_C$ | 6845 | 6868 | 7060 | 6979 | 7034 |

In order to get better insight into the physical background of the stress components we determined the activation energy of the relaxation processes by means of the creation of the master curve. According to our previous works [13,14], the creation of the master curve by horizontal shift of the relaxation curves measured at different test temperature can be applied only for the relaxing stress component $\Delta\sigma(t)$. The stress relaxation curves $\sigma(t)$ were subtracted by the non-relaxing stress component $\sigma_\infty$ resulting in the relaxing stress component $\Delta\sigma(t)$ according to Eq. (1). The relaxing stress curves $\Delta\sigma^V(t)$ and $\Delta\sigma^{Comp}(t)$ of the unfilled vulcanizate V and the composite C91, respectively, are presented in Fig. 11a and b. As discussed above (Fig. 8a) the relaxing stress component $\Delta\sigma^V$ is not dependent on the temperature, thus, in Fig. 11a all curves $\Delta\sigma^V(t, T)$ overlap each other. Deduced from that the shift of the relaxation curves of $\Delta\sigma^{Comp}(t, T)$ toward lower level with increasing temperature is merely caused by the contribution of the CB.

By creation of the master curve of the composite C91 the curves $\Delta\sigma^{Comp}(t, T)$ presented in Fig. 11b were shifted horizontally toward the curve measured at the reference temperature $T_R = 30$ °C. It was found that only the curve measured at 50 °C is well fitted to the curve measured at $T_R = 30$ °C while the curves measured at 90 °C and 110 °C fit to the curve measured at 70 °C very well. It is noteworthy that the curve measured at 70 °C intersects the curve measured at 50 °C. That indicates a change of relaxation mechanisms when the test temperature exceeds 70 °C. In Fig. 12b two master curves at reference temperature of 30 °C and 70 °C were originated by different relaxation mechanisms. The same result was found for all investigated composites as seen in Fig. 12a,c and d. The position of the master curve with $T_R = 30$ °C is the same for three composites, but the master curve with $T_R = 70$ °C shifts to lower level with increasing CB dispersion.

In order to identify the physical background of the relaxing stress component the horizontal shift factor $a_T$ of all composites

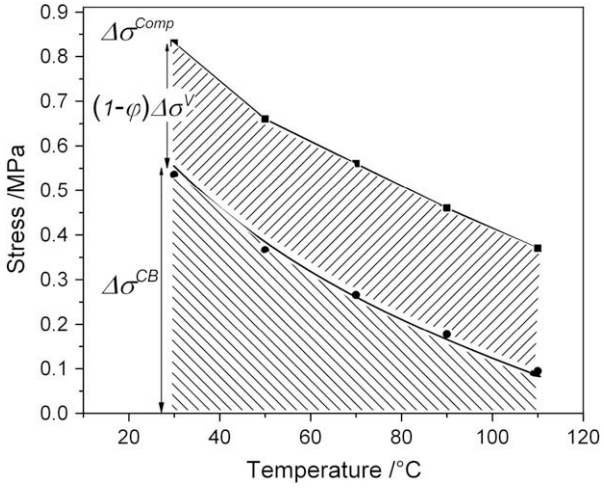


**Fig. 9.** Relaxing stress component $\Delta\sigma^M = (1-\varphi)\Delta\sigma^V$ of the matrix and $\Delta\sigma^{CB}$ of CB in the composite C91 in dependence on the test temperature.

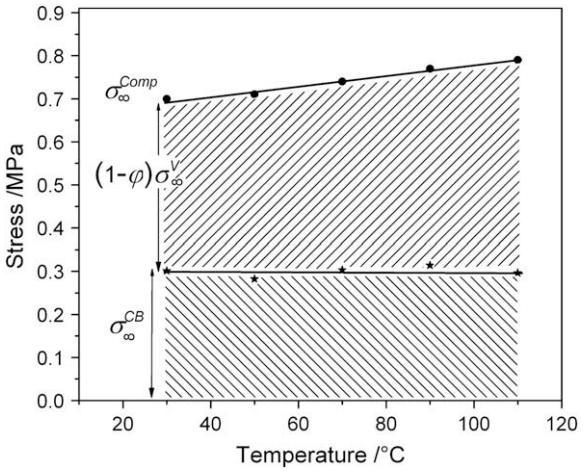


**Fig. 10.** Non-relaxing stress component $\sigma_\infty^M = (1-\varphi)\sigma_\infty^V$ of the matrix and $\sigma_\infty^{CB}$ of CB in the composite C91 in dependence on the test temperature.

was presented in dependence on the reciprocal temperature as shown in Fig. 13a. We recognize two temperature ranges I and II within them the temperature dependence of $\log a_T$ can be described by the Arrhenius equation [31]. Up to 50 °C all the composites have the same temperature dependence of $\log a_T$. The activation energy $E_A = 79$ kJ/mol was calculated from the slope of the straight line according to the Arrhenius equation. It is independent of the state of CB network built-up in the composites. Thus the main relaxation process in the temperature range up to 50 °C is assumed as the time dependent debonding (desorption) of the bonds between the nitrile group of NBR and the active centers available on the CB surface. The contribution of this process to the stress $\Delta\sigma^{CB}$ is denoted as $\Delta\sigma^{CB(rubber\text{-}layer)}$. The debonding process was computerized in different works [32,33] using finite element methods. Using the unit cell model containing four spherical CB particles, Matouš and Geubelle [32] revealed that the debonding is first detected at the pole of a particle due to the stress concentration. The debonding of particle leads to the unloading of this matrix region, and the next debonding is generated in the vicinity of the nearest particle. These debonding events take place in a relatively progressive fashion. Lu and Tomita [33] also used the cohesive zone model [34] to describe the process of debonding around carbon black. At a critical stress-state, void nucleation occurs inside the less mobile bound rubber and leads to the onset of debonding around carbon black, which is important to the deformation resistance, hysteresis loss and the volume dilatation of carbon black filled rubber. The work also clarified the effects of critical interfacial strength and the characteristic length, and volume fraction of carbon black as well as heterogeneity of the density of molecular chains around carbon black on the debonding processes.

In the temperature range above 70 °C composites show different temperature dependence of the shift factor $a_T$. The slope of the straight line decreases with increasing dispersion degree $D$, e.g. from C79 to C97. Due to the increase of the test temperature new rubber–filler bonds can be produced by reorganization processes in the rubber-layer [35] and they become more stable with time. The debonding as a main process in the temperature region up to 50 °C becomes insignificant in the subsequent temperature range. The new mechanism controlling the stress relaxation process now correlates well to the state of the CB network.

According to the well-known *Payne-effect* [36] a sudden decrease of the storage modulus at a small dynamic strain is a result

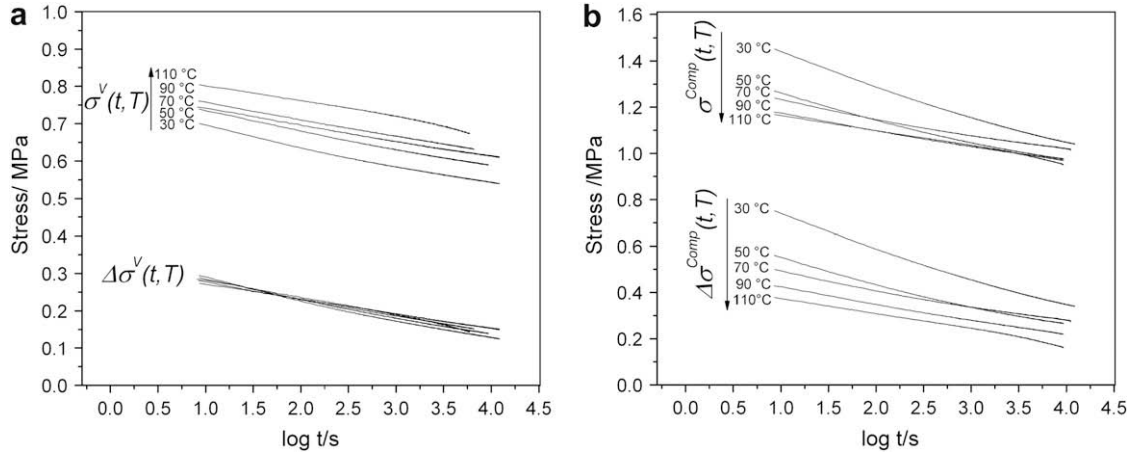


**Fig. 11.** Relaxing stress curves $\Delta\sigma^{V}(t, T)$ and $\Delta\sigma^{Comp}(t, T)$ of the unfilled vulcanizate V (a) and composite C91 (b), respectively, after subtraction of the non-relaxing component $\sigma_\infty$ from the relaxation curves $\sigma^{V}(t, T)$ and $\sigma^{Comp}(t, T)$.

of the breakage and reforming of physical (van der Waals) bonds between filler aggregates that were assumed to build an energetically elastic filler network within the soft rubber matrix. At large strains this filler network breaks down and the elastic stress is then determined only by rubber–rubber cross-links, elastically effective filler–polymer couplings and hydrodynamic filler effects. In contrast, the model of flexible chain aggregates [37] implied that the main contribution of the elastic energy in the strained filler clusters results from the bending–twisting deformation of filler–filler bonds. The typical non-linear viscoelastic behavior of reinforced rubbers with the pronounced stress softening and hysteresis results mainly from a break-down and re-aggregation of the filler network at large strain amplitudes [38]. This mechanism involves both the elastic properties and the failure properties of filler–filler

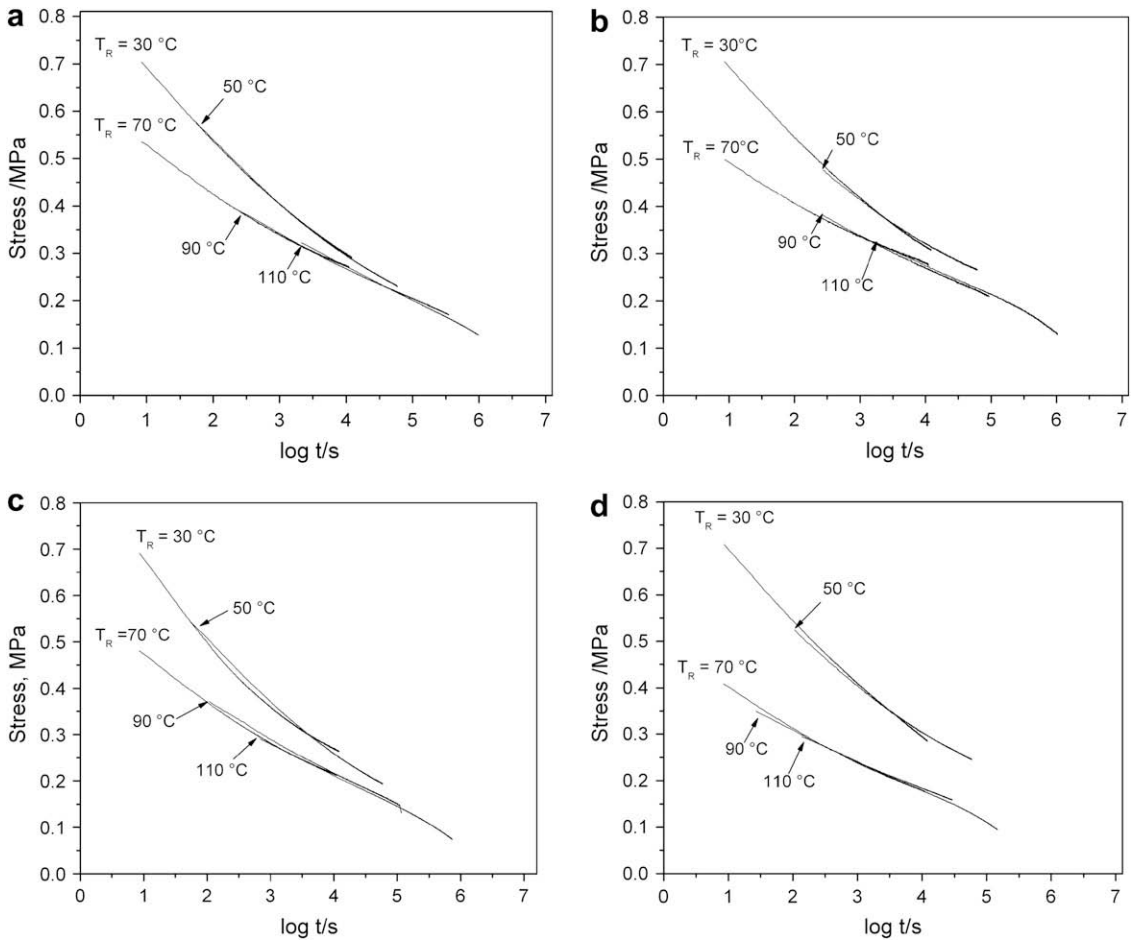


**Fig. 12.** Master curve of the relaxing stress component $\Delta\sigma^{Comp}(t, T)$ of different composites, C79 (a), C91 (b), C95 (c) and C97 (d).

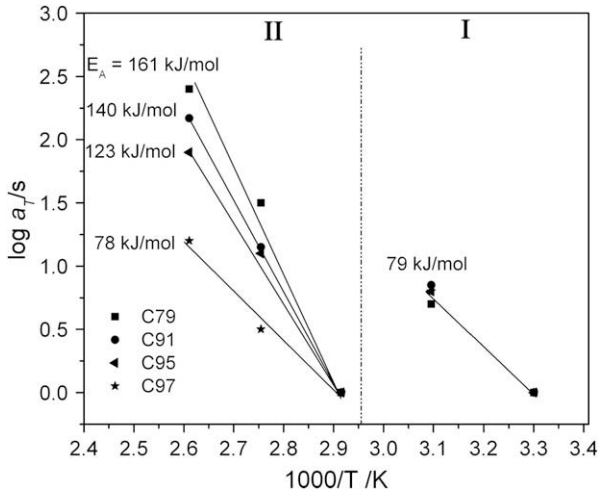


**Fig. 13.** Temperature dependence of the shift factor $a_T$ of different composites.

bonds and agglomerates in dependence on agglomerate size. As seen in Fig. 3a the CB network of C79 is still not developed with large agglomerates. The filler–filler bonds within the robust agglomerates are hard to be collapsed with time. A high activation energy of about 161 kJ/mol for C79 was found. With better CB dispersion the CB network becomes looser and flaky which is easier to be destroyed with time. The determined activation energy decreases from 161 kJ/mol to 78 kJ/mol with increasing CB dispersion that indicates that the new relaxation process is accelerated in the order C79, C91, C95 and C97. Vennemann [6] suggested that an increase in temperature would further aid in weakening filler–filler bonds. Thus in the present work the collapse of the bending–twisting deformed filler–filler bonds is supposed as the new relaxation process taking place when test temperature exceeds 70 °C. The relaxing stress contribution resulted from the collapsed filler network is named $\Delta\sigma^{CB(network)}$. As seen in Fig. 12a–d the master curve at reference temperature of 70 °C shifts more strongly downwards when the CB macrodispersion increases.

In Fig. 14 the non-relaxing stress component $\sigma_\infty^{CB}$ is presented in dependence on the CB dispersion. It increases with CB dispersion and reaches a maximal value at a dispersion of 91% (composite

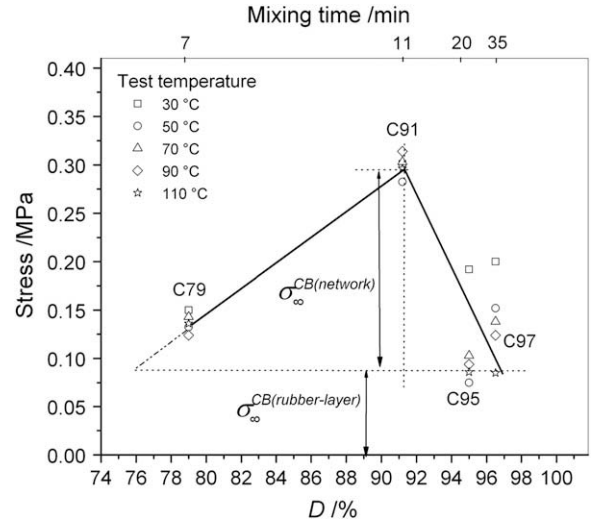


**Fig. 14.** Non-relaxing stress component $\sigma_\infty^{CB}$ measured at different temperature in dependence on the dispersion degree $D$.

C91), after that it decays to the same level of C79. The change of the $\sigma_\infty^{CB}$ is as similar as the online measured electrical conductance (compared to Fig. 4) that let us conclude that the stress component $\sigma_\infty^{CB}$ is dependent on the state of the CB network. In C79 the CB network is not yet developed and in C97 the CB network is destroyed due to the excessive mixing. The number of the stable filler–filler bonds in both samples is low. We assume that the contribution $\sigma_\infty^{CB(network)}$ in the composites C79 and C97 is nearly zero and in C91 maximal. The difference resulted from $\sigma_\infty^{CB}$ and $\sigma_\infty^{CB(network)}$ is a constant value which is not dependent on the CB dispersion and state of CB network. According to Fig. 4 the rubber-layer $L$ reaches a plateau at a dispersion of 76%. All investigated composites have the same value of $L$. Thus, the constant stress value resulted from difference between $\sigma_\infty^{CB}$ and $\sigma_\infty^{CB(network)}$ is suggested as the contribution of the time-stable rubber–CB bonds available in the rubber-layer. It can be denoted as $\sigma_\infty^{CB(rubber\text{-}layer)}$. The result is the same for all investigated temperatures.

## 4. Conclusions

The stress relaxation behavior of rubber–CB composites was characterized by use of a new evaluation method. The initial stress was divided into several stress components and the structure of the investigated polymer system was considered as a combination of different networks. By means of this new experimental strategy a structural characterization of the stress relaxation behavior of rubber–CB composites has been done by taking into account the effect of CB dispersion degree. Thus, the mechanical performance of the CB filled rubber composites and especially their time and temperature dependent mechanical behavior could not only better to be understood, but the results deliver the basis for a more targeted development and application of rubber–CB composites.

## Acknowledgement

The authors wish to thank the German Research Foundation (DFG) for the financial support.

## References

[1] Ghosh AK, De D, Adhikari B. Kautsch Gummi Kunstst 1998;51:500–3.
[2] Takino H, Iwama S, Yamada Y. Rubber Chem Technol 1997;70:15–24.
[3] Hess WM, Herd CR, Sebok EB. Kautsch Gummi Kunstst 1994;47:328–41.
[4] Berry JP, Watson WF. J Polym Sci 1955;18:201–13.
[5] Ronan S, Alshuth T, Jerrams S. Kautsch Gummi Kunstst 2007;60:559–63.
[6] Srinivasan N, Bökamp K, Vennemann N. Kautsch Gummi Kunstst 2005; 58:650–5.
[7] Mahapatra SP, Sridhar V, Chaudhary RNP, Tripathy DK. Polym Eng Sci 2007;47:984–95.
[8] Sridhar V, Chaudhary RNP, Tripathy DK. J Appl Polym Sci 2006;101:4320–7.
[9] Seeger A. Handbuch der Physik. Berlin: Springer; 1958.
[10] Seeger A. Z Naturforsch 1954;9a:758, 856, 870.
[11] Krausz AS, Eyring H. Deformation kinetics. New York: Wiley; 1975.
[12] Ferry JD. Viscoelastic properties of polymers. New York: Wiley; 1980.
[13] Le HH, Lüpke Th, Pham T, Radusch H-J. Polymer 2003;40:4589–97.
[14] Le HH, Zia Q, Ilisch S, Radusch H-J. Expr Polym Lett 2008;2(11):791–9.
[15] Le HH, Prodanova I, Ilisch S, Radusch H-J. Rubber Chem Technol 2004;77: 815–24.
[16] Le HH, Ilisch S, Kasaliwal GR, Radusch H-J. Kautsch Gummi Kunstst 2007; 60:241–8.
[17] Le HH, Ilisch S, Steinberger H, Radusch H-J. Plast Rubber Comp Macromol Eng 2008;37:367–75.
[18] Stumpe NA, Railsback HE. Rubber World 1964;151:41–3.
[19] Astm D 2663: standard test methods for carbon black-dispersion in rubber.
[20] Le HH, Ilisch S, Kasaliwal G, Radusch H-J. Rubber Chem Technol 2008;81: 767–81.
[21] Li JCM. Can J Phys 1967;45:493.
[22] Shiga S, Furuta M. Rubber Chem Technol 1985;58:1–22.
[23] Li Q, Feke DL, Manas-Zloczower I. Rubber Chem Technol 1995;68:836–41.
[24] Yamada H, Manas-Zloczower I, Feke DL. Rubber Chem Technol 1997;71:1–16.
[25] Seyvet O, Navard P. J Appl Polym Sci 2001;80:1627–9.
[26] Kraus G. Adv Polym Sci 1971;8:155–237.

[27] Rivin D. Rubber Chem Technol 1971;44:307–43.
[28] Donnet JB, Voet A. Carbon black, physics, chemistry and elastomer reinforcement. New York: Marcel Dekker; 1976 [chapter 8].
[29] Treloar LRG. The physics of rubber elasticity. 3rd ed. Oxford: Clarendon Press; 1975.
[30] Isono Y, Ferry JD. Rubber Chem Technol 1984;57:925–43.
[31] Glasstone S, Laidler KJ, Eyring H. The theory of rate process. New York: McGraw-Hill; 1941.
[32] Matouš K, Geubelle PH. Int J Numer Meth Eng 2006;65(2):190–223.
[33] Lu W, Tomita Y. In: WCCM VI in conjunction with APCOM'04, Sept. 5–10, Beijing, China; 2004.
[34] Needleman AJ. Appl Mech 1987;54:525–31.
[35] Choi SS. Polym Adv Technol 2002;13(6):466–74.
[36] Payne AR. J Appl Polym Sci 1960;3:127.
[37] Kantor Y, Webman I. Phys Rev Lett 1984;52:1891–4.
[38] Klüppel M. Adv Polym Sci 2003;164:1–86.